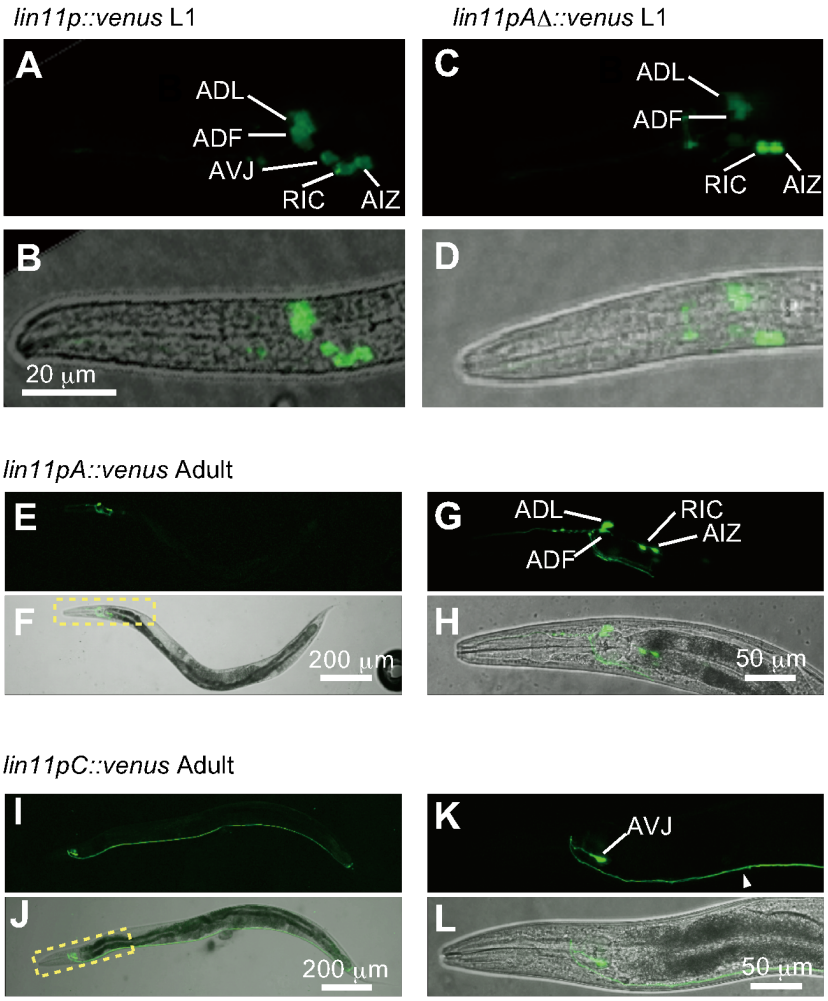

Figure S1 Expression patterns of synthetic promoters. (A-D) Fluorescent reporter expression by *lin-11p::venus* (A and B) and *lin-11pAΔ::venus* (C and D) in the head region of L1 larvae. The fluorescence images (A and C) and images merged with bright field images (B and D) are shown. (E-L) Fluorescent reporter expression by *lin-11pA::venus* (E-H) and *lin-11pC::venus* (I-L) at adult. The fluorescence images (E, G, I, and K) and images merged with bright field images (F, H, J, and L) are shown. G, H, K, and L are magnified images of the region surrounded by yellow squares in F or J.

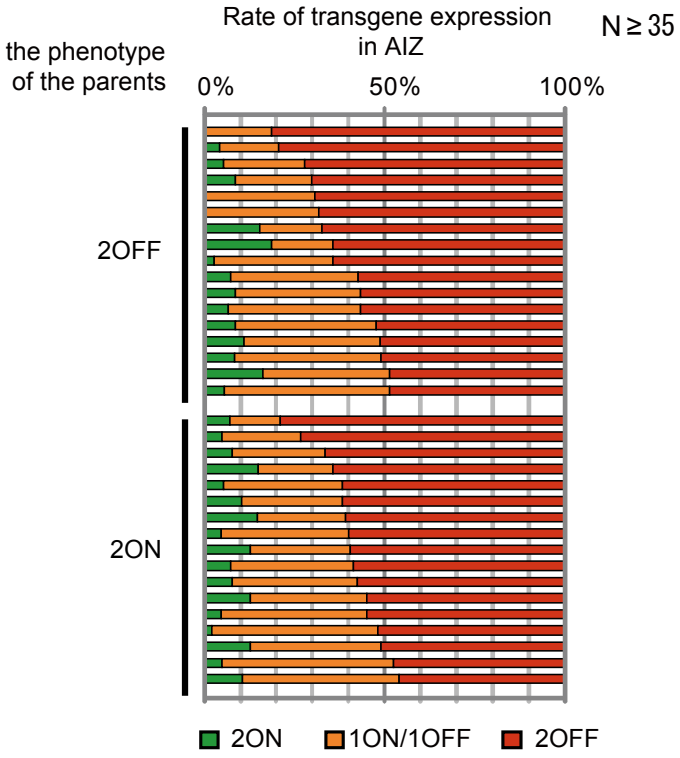

Figure S2 AIZ phenotypes of individual populations of offspring from isolated *peIs304* animals. 17 *peIs304* animals with AIZ-2ON and AIZ-2OFF phenotypes were separately isolated. Each animal was self-fertilized and the progeny were tested for the AIZ phenotypes at adult. The distribution of phenotypes is shown for each population. (N ≥ 35 for each population)

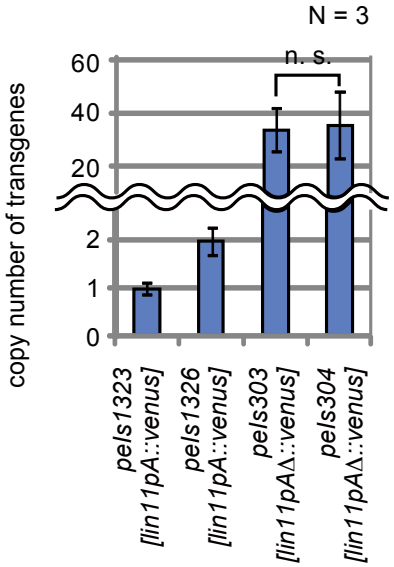

Figure S3 Copy number of reporter transgenes in the chromosomally integrated transgenes. The relative copy numbers of transgenes were quantified by performing real-time PCR against a sequence in the *venus* gene and the sequence in the *pqe-1* gene in the genome for control. The relative copy numbers were further normalized by that of *peIs1323[lin-11pA::venus]* which was supposed to be a single-copy insertion. (N = 3, Error bars represent the S.E.M., n.s. indicates that they are not significantly different at $P < 0.01$ by Student's t test)

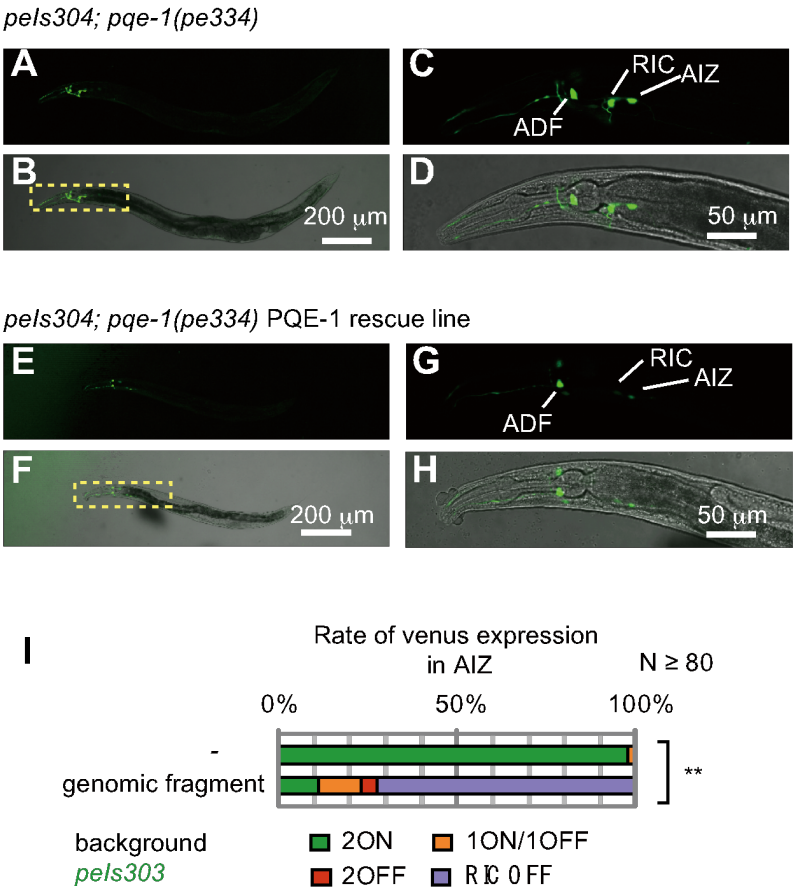

Figure S4 Overexpression of *pqe-1* represses the reporter expression also in RIC neurons. (A-H) Expression pattern of peIs304 with (E-H) or without (A-D) a rescuing transgene *H20p::pqe-1C.* The fluorescence images (A, C, E, and G) and images merged with bright field images (B, D, F, and H) are shown. C, D, G, and H are magnified images of the region surrounded by yellow squares in B or F. For E-H, an animal with typical RIC OFF phenotype was picked.

(I) AIZ phenotype of *peIs303* animals with overexpression of *pqe-1*. The extrachromosomal array which consists of genomic fragment of *pqe-1* was transferred to wild-type *peIs303* background from a rescue line of *pqe-1(pe334); peIs304* by a cross. The extrachromosomal array only with transformation marker *myo-3p::mRFP* was also transferred to the *peIs303* background and used as control. Only the animals that carried the extrachromosomal array were used for the analysis. (N ≥ 60, ** shows significant differences at $P < 0.001$ by Chi-square test.)

A

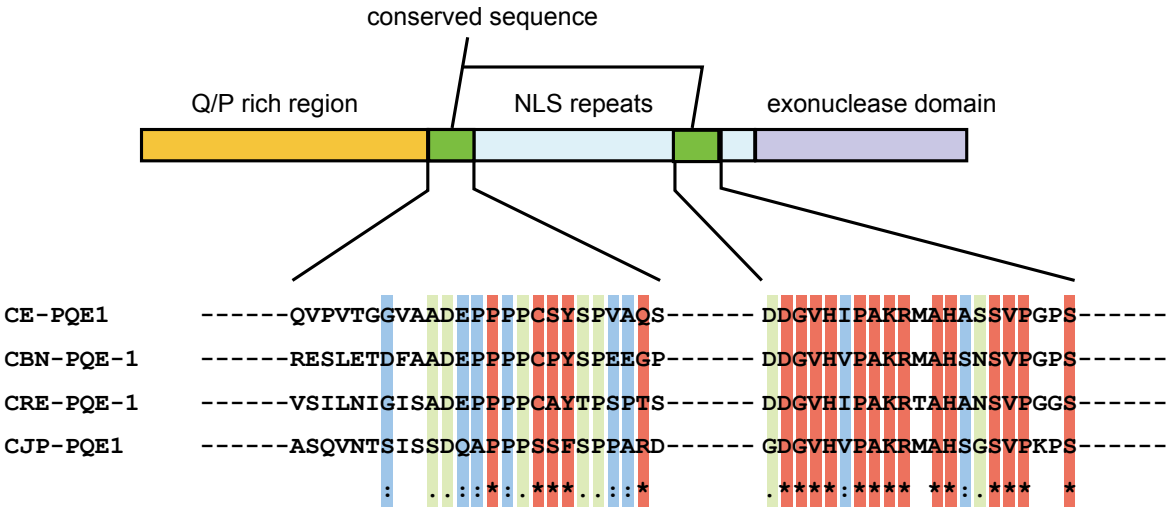

B

The rate of glutamine(Q) and proline(P) in the Q/P rich region

	total a.a.	Q	P	Q rate	P rate
CE	572	112	89	0.20	0.16
CBN	614	126	112	0.21	0.18
CRE	572	115	70	0.20	0.12
CJP	383	72	49	0.19	0.13

Figure S5 Domain structure of the PQE-1 protein. (A) An illustration of the domain structure of the PQE-1A protein. The PQE-1A isoform has a Q/P rich region, NLS repeats with conserved sequences, and an exonuclease domain. Two short sequences are well conserved in PQE-1 proteins of Caenorhabditis species (CE: elegans, CBN: brenneri, CRE: remanei, CJP: japonica) and are included in PQE-1A and PQE-1C isoforms. (*, :, and . indicate fully conserved residue, conservation of a 'strong group', and conservation of a 'weak group', respectively, which are defined in ClustalW.) (B) Number and the content of glutamine, Q, and proline, P, residues in Q/P rich region.

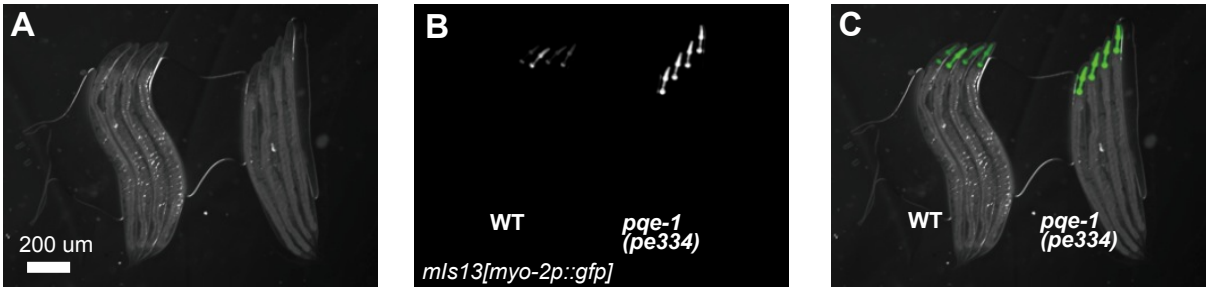

Figure S6 Enhancement of transgene expression by the pqe-1 mutation. (A-C) Enhancement of the expression from *mIs13[myo-2p::gfp]* by *pqe-1(pe334)* mutation. The bright field image (A), fluorescence image (B), and merged image (C) of *mIs13* animals in wild-type and *pqe-1(pe334)* mutant background are shown. Four animals for each genetic background are aligned.

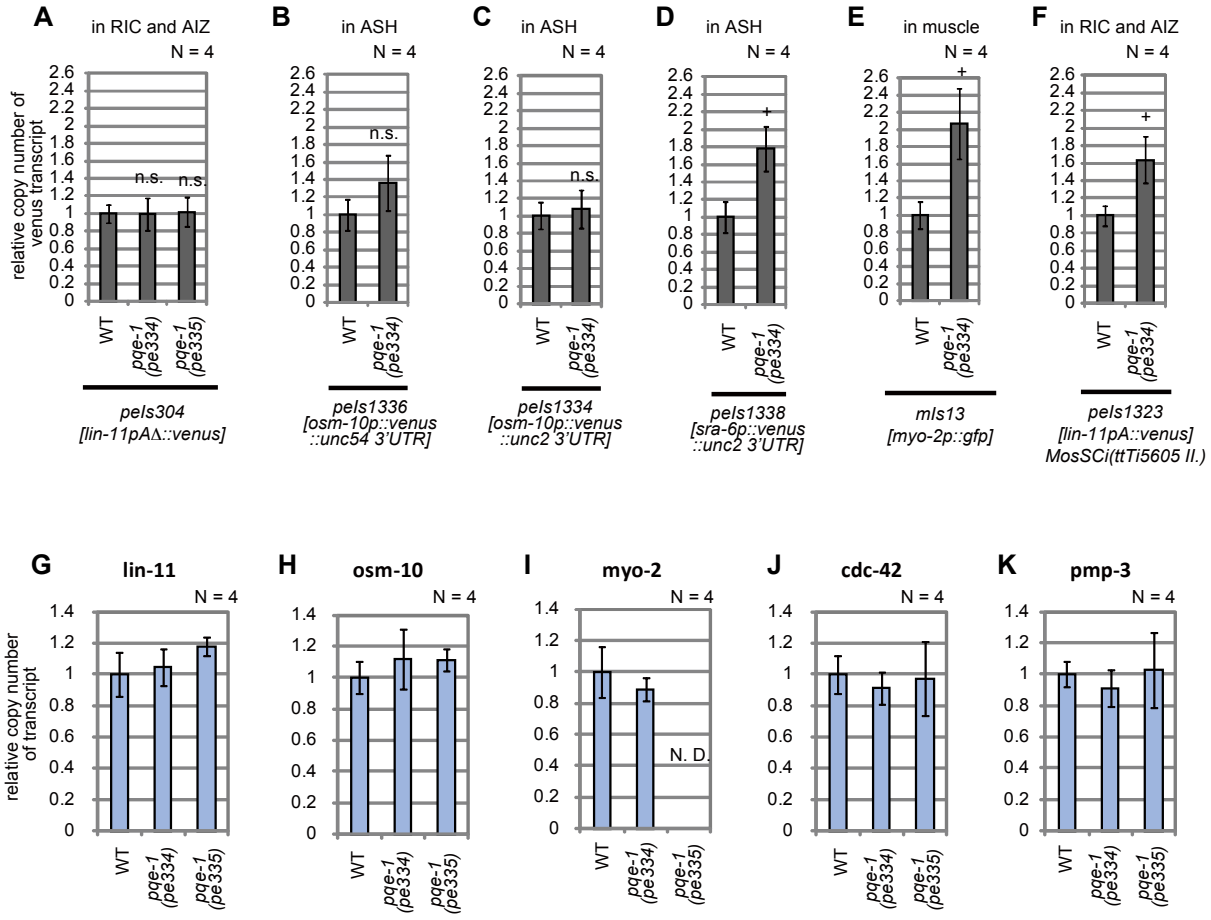

Figure S7 Quantification of transcripts from L1 larava. (A-F) The copy numbers of venus transcripts were quantified by real-time PCR following reverse transcription. Normalized numbers of transcripts from *peIs304[lin-11pAΔ::venus]*, *peIs1336[osm-10p::venus::unc-54 3'UTR]*, *peIs1334[osm-10p::venus::unc-2 3'UTR]*, *peIs1338[sra-6p::venus::unc-2 3'UTR]*, *mIs13[myo2p::venus]*, and *peIs1323[lin-11pA::venus]*(MosSCI) are shown in (A-F), respectively. (G-K) The copy numbers of transcripts of intrinsic genes were quantified by real-time-PCR following reverse transcription. Normalized numbers of transcripts from *lin-11*, *osm-10*, *myo-2*, *cdc-42*, and *pmp-3* are shown in (G-K), respectively.

(N = 4, N. D. indicates that the result is Not Determined., Error bars represent the S.E.M., + shows significant difference at $P < 0.05$ and n.s. indicates that they are not significantly different at $P < 0.05$ by Student's t-test)

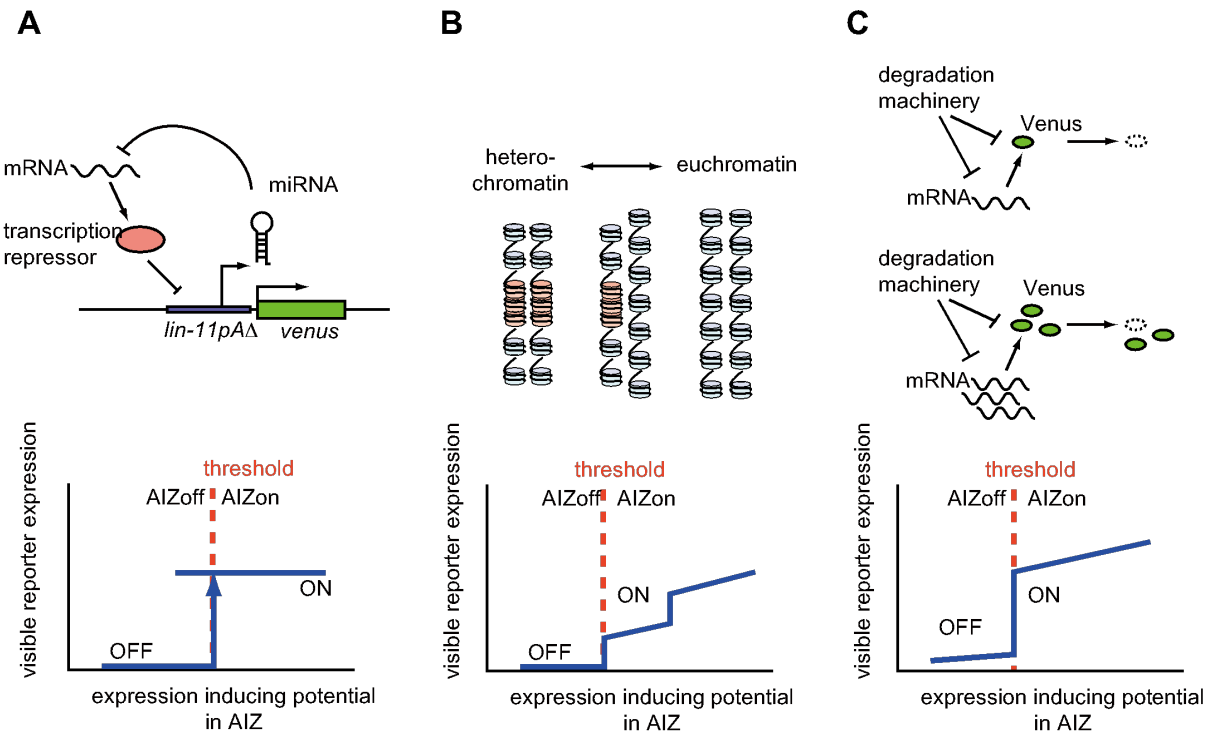

Figure S8 Models for stochastic reporter expression in AIZ neurons. (A) A model with bistable gene regulation system. In this model, double negative feedback loop can be formed by hypothesizing a miRNA that is encoded in the promoter region and interfere with the expression of a transcription repressor. (B) A model by chromatin conformation switching. In this model, the conformation of chromatin switches between heterochromatin and euchromatin, while the selected state is fixed after development. Because each cell has two transgenes on the homologous chromosomes, intermediate expression state should appear. (C) A model by a constant degradation mechanism. If the level of reporter transcription is fixed during development, the rate of degradation of transcripts or proteins can define the minimum level of expression induction required for expression of the reporter.